COMPARISON OF ONE- AND TWO-DIMENSIONAL FLOOD MODELING IN URBAN ENVIRONMENTS

SULOCHAN DHUNGEL[1], MICHAEL E. BARBER[1] & ROBERT L. MAHLER[2]
[1] Civil and Environmental Engineering, University of Utah, Salt Lake City, UT, U.S.A.
[2] Soil Science Division, University of Idaho, Moscow, ID, U.S.A.

ABSTRACT
The US Army Corps of Engineers Hydrologic Engineering Center recently released version of the River Analysis System (HEC-RAS) has added two-dimensional (2D) modeling capabilities to a decade old one-dimensional (1D) model dating back to HEC-2 developed in the 1970s. Several recent studies have indicated that 2D flood modeling is preferable in urban environments to better account for the complex topography caused by infrastructure. The newest version of HEC-RAS also allows users to simulate unsteady flow using either the Saint Venant equations or the diffusion wave (DW) equations using an implicit finite volume algorithm. The Saint Venant solution allows for turbulence and Coriolis effects to be accounted for with momentum additions. While applicable to a wider range of flood problems, the Saint Venant solution is slower and inherently less stable than the DW approach. We evaluate the similarities and differences between both 1D and 2D solution techniques using the lower Provo River in Utah as a prototypical urban river. Furthermore, since the 2D version of HEC-RAS is relatively new, we compared the HEC-RAS simulations to the 2D sedimentation and river hydraulics (SRH-2D) model developed by the U.S. Bureau of Reclamation. The method uses high resolution light detection and ranging imagery to determine floodplain topography and cross-section information for the channel properties. While no single river reach can adequately answer the question of whether 2D flood modeling produces superior results compared to 1D solutions, in this study the 1D unsteady flow model struggled to predict meandering stream phenomenon particularly because it was difficult to identify active flow versus storage areas as a function of flow depth. We conclude that temporal variations in most complex flow regimes will not be well modeled in 1D and that 2D modeling will produce superior results.
Keywords: HEC-RAS, LiDAR, mesh generation, overbank storage, SRH-2D.

1 INTRODUCTION

Accurate flood modeling is essential in the face of increases in urbanization and the frequency of extreme climate events. This need, coupled with increased computing power and improved access to high-resolution data, has led to the growing ability of modeling complex flood flows with more detail than was previously possible [1], [2]. Increasingly, two-dimensional (2D) models are supplanting traditional one-dimensional (1D) approaches incorporating GIS and remote sensing data. While studies are beginning to examine the similarities and differences between these models [3], the specific complex nature of local conditions will require a large number of case studies to begin to completely understand situations where one approach is superior to the other given data and budget constraints and multiple project goals. There have been numerous studies concluding that 2D models are superior or at least equal to 1D models which, given unlimited budgets for data collection, calibration, and sufficient modeling expertise, would seem rather obvious [4]–[6]. However, as concluded by Gibson and Pasternack [7], the most important questions revolve around how much better and at what additional cost? These are critical issues that will not be easily addressed but the goal of this study is to add to the increasing body of knowledge related to these questions.

2 BACKGROUND

Because of the importance of accurately delineating floodplains for protection of property and human lives throughout the world, numerous 1D, 2D, and three-dimensional (3D) flood

ISSN: 1743-7601 (paper format), ISSN: 1743-761X (online), http://www.witpress.com/journals
DOI: 10.2495/SDP-V14-N4-356-366

forecasting models have been developed [8]–[11]. In this study, we examine the 2D modeling algorithm, now included in the River Analysis System (HEC-RAS) model developed by the U.S. Army Corps of Engineers Hydrologic Engineering Center, in comparison to the original 1D approach and the 2D sedimentation and river hydraulics (SRH-2D) model developed by the U.S. Bureau of Reclamation. These models were selected because they are widely used and freely distributed.

2.1 Overview of model formulations

HEC-RAS 1D uses the Newton–Raphson iteration technique to solve the 1D Saint Venant equations written to account for channel and floodplain flows. The continuity and momentum equations are [3], [12]:

$$\frac{\partial Q}{\partial t}+\frac{\partial(\varnothing Q)}{\partial x_c}+\frac{\partial\left((1-\varnothing)Q\right)}{\partial x_f}=0 \tag{1}$$

$$\frac{\partial Q}{\partial t}+\frac{\partial\left(\frac{\varnothing^2 Q^2}{A_c}\right)}{\partial x_c}+\frac{\partial\left(\frac{(1-\varnothing^2)Q^2}{A_f}\right)}{\partial x_f}=-gA_c\left(\frac{\partial z}{\partial x_c}-S_{fc}\right)-gA_f\left(\frac{\partial z}{\partial x_f}-S_{ff}\right) \tag{2}$$

where g is gravity, t time, x_c the longitudinal distance along the main channel, x_f the distance along the floodplain cross sections, z the water surface elevation, A_c the channel area, A_f the floodplain area, Q the total flow, S_{fc} the channel friction slope, S_{ff} the floodplain friction slope, and ø the main channel flow portion of the total flow.

HEC-RAS 2D and SRH-2D are based on the vertically averaged 3D Navier–Stokes equations that produces the standard 2D Saint Venant equations for continuity and momentum in the form of [12], [13]:

$$\frac{\partial h}{\partial t}+\frac{\partial(hu)}{\partial x}+\frac{\partial(hv)}{\partial y}=e \tag{3}$$

$$\frac{\partial(hu)}{\partial t}+\frac{\partial\left(hu^2\right)}{\partial x}+\frac{\partial(huv)}{\partial y}=\frac{\partial\left(hT_{xx}\right)}{\partial x}+\frac{\partial\left(hT_{xy}\right)}{\partial y}-gh\frac{\partial z}{\partial x}-\frac{\tau_{bx}}{\rho}+D_{xx}+D_{xy} \tag{4}$$

$$\frac{\partial(hv)}{\partial t}+\frac{\partial(huv)}{\partial x}+\frac{\partial\left(hv^2\right)}{\partial y}=\frac{\partial\left(hT_{xy}\right)}{\partial x}+\frac{\partial\left(hT_{yy}\right)}{\partial y}-gh\frac{\partial z}{\partial y}-\frac{\tau_{by}}{\rho}+D_{yx}+D_{yy} \tag{5}$$

where e is the excess rainfall rate, g the gravity, h the water depth, t time, x the longitudinal axis, y the transverse axis, u and v the depth-averaged flow velocities in the x and y directions, T_{xx}, T_{xy}, and T_{yy} the depth-average turbulent stresses, D_{xx}, D_{xy}, and D_{yy} the dispersion terms due to depth averaging, τ_{bx} and τ_{by} the bed shear stresses, ρ the water density, and z the water surface elevation (bed elevation + h).

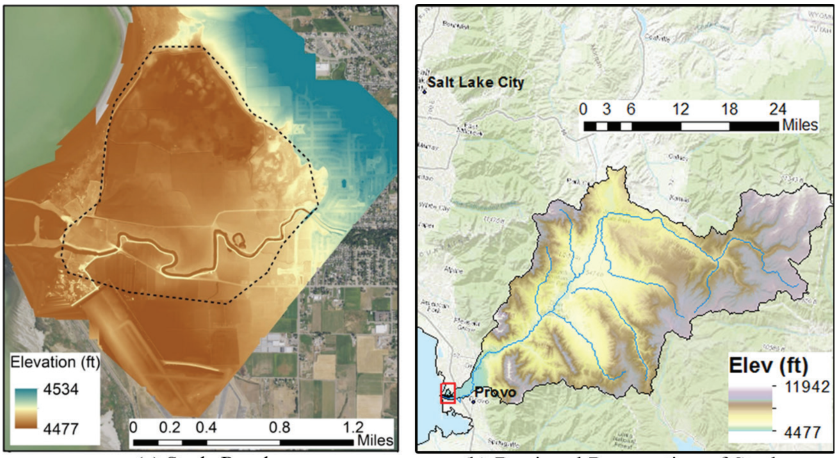

(a) Study Reach

(b) Regional Perspective of Study Location

Figure 1: Study area. (a) Provo river study reach; (b) Provo river, Utah location within the U.S.

2.2 Case study: Provo river watershed in Provo, UT

The lower Provo river was used as our study area (see Fig. 1). The 1,740 km^2 Provo river watershed originates in the Uinta Mountains and terminates in Utah Lake. The 110 km long river begins at an elevation of nearly 3,000 m and discharges into the lake at an elevation of 1,370 m. The lower portion of the river, however, is far less steep as it exits the canyon and travels through the City of Provo.

3 METHODOLOGY

3.1 Modeling approach

Using the Provo river study area described above, we conducted the following model runs:

1. HEC-RAS 1D with a storage area
2. HEC-RAS 2D with full momentum (FM) and diffusion wave (DW) approximation
3. SRH 2D with FM

Floodplain information was derived from high resolution light detection and ranging (LiDAR) imagery to determine floodplain topography and cross-section information for the channel properties.

As illustrated in Fig. 2, HEC-RAS 1D model uses a storage area connected to the river assuming a broad crested weir relationship exists at the cross-section/storage area interface.

The SRH-2D model is based on the 2D depth-averaged dynamic wave equations using a finite-volume numerical solution method [5]. For this study, the model was coupled with the SMS graphical user interface developed by Aquaveo™. Rather than the rectangular grid employed by the HEC-RAS 2D model as shown in Fig. 3a, this model allows for triangular-shaped elements in either a normal grid option or an optimized grid based on gradients (shown in Fig. 3b).

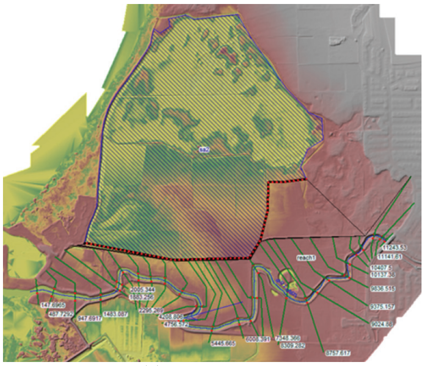

(a) Storage area.

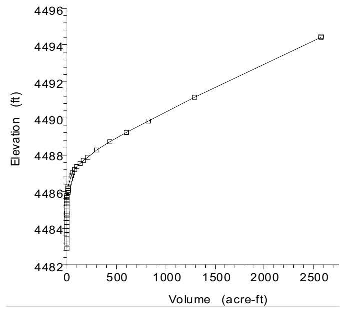

(b) Stage-volume curve for storage area.

Figure 2: One-dimensional layout of HEC-RAS model with (a) storage area and (b) stage-storage volume relationship.

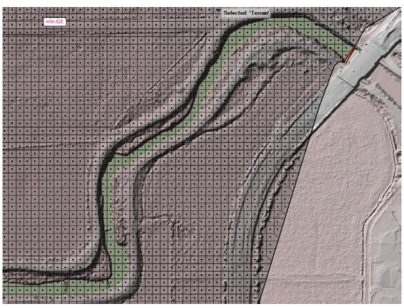

(a)Basic gridding in HEC-RAS

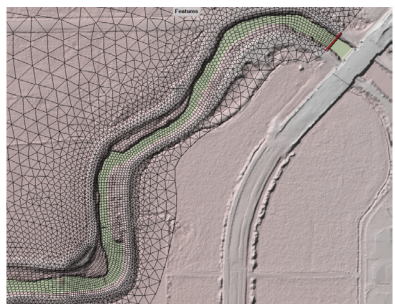

(b)Optimized gridding using SMS

Figure 3: Mesh creation for 2D models.

The models require a hydrograph (or flow when modeling steady state) as an upstream boundary condition and lake elevation as a downstream boundary condition for this stream (Fig. 4(a)). We used the flow data from the USGS Station '10163000 Provo River',

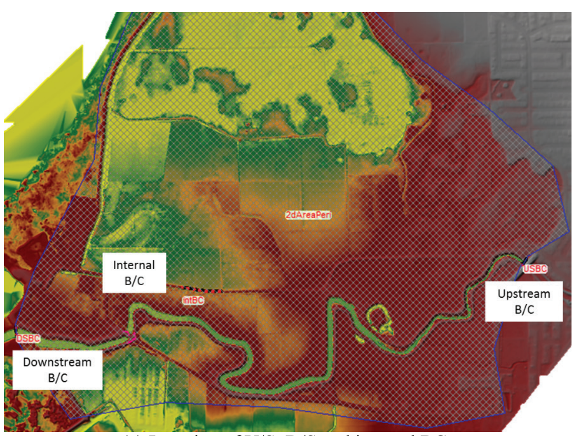

(a) Location of U/S, D/S and internal BCs

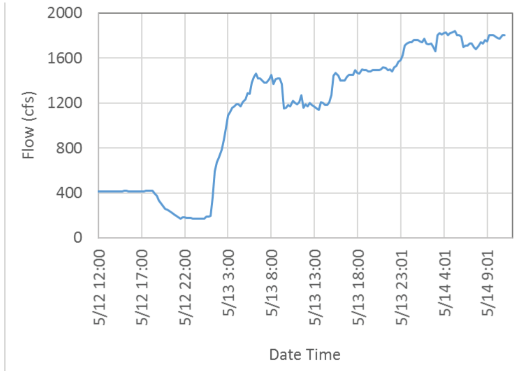

(b) U/S boundary condition flow

Figure 4: Upstream inflow hydrograph.

0.7 miles upstream from the upstream boundary of the model. The event that produced flooding conditions in our study occurred between May 12, 2017, 11:00 AM to May 14, 2017, 11:00 AM as shown in Fig. 4. Since the bathymetry was not accurately represented in the LiDAR dataset, the flow area was underestimated. To account for that, we reduced the overall flow by 75% based on differences in elevation from the field survey and LiDAR. For the downstream boundary condition, we chose a constant lake elevation of 4489 ft. Additionally, we used an internal boundary condition at the lowest point of the weir to measure breach flow.

Manning's n was chosen to be 0.08 for the overbank flows and 0.03 for the channel flow.

4 RESULTS AND DISCUSSION

4.1 Comparison of HEC RAS 1D and 2D model results

HEC RAS model results at the D/S boundary conditions for different model runs are presented in Fig. 5a. All the models capture the reduction in outflow due to reduction in inflow at around May 12, 2:15 AM consistently, which indicates consistency in flood routing mechanisms between the models. However, we see that the magnitude of flows varies significantly between different model runs. The highest outflow is observed for 2D model with 25 ft grid size and a computational time step of 1 s with DW approximation approach, while the lowest outflow was observed for 2D model with 10 ft grid size and computational time step of 5 s with FM approach.

To understand some of these differences in flow at the downstream boundary conditions, flow values through the weir into the storage area were also compared as shown in Fig. 5b. The timings of breach were different for different models. The breach of the weir for 1D model occurred at May 13, 4:45 AM. This timing was similar to the 2D model with coarse resolution of 25 feet. However, for the model with finer grid size (10 ft), two breach events occurred and the latter breach event's timing was about 2 h earlier when compared to 1D model results. Since the water flowing into the storage area does not return to the downstream end, differences in flow values at the downstream boundary were observed. Additionally, in the model with a grid size of 25 ft, the weir is not well represented and missed the first breach as observed in model with grid size of 10 ft.

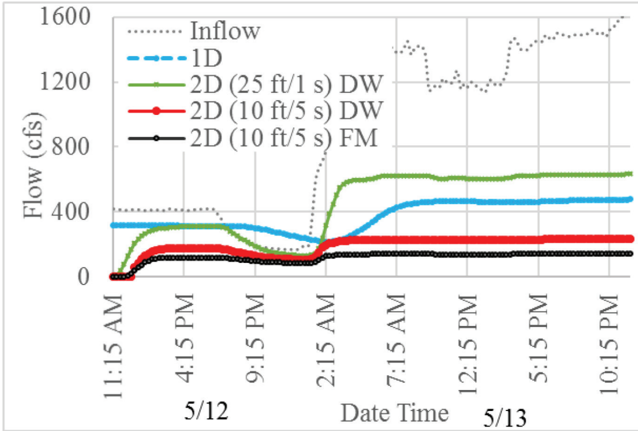

(a) Downstream Boundary

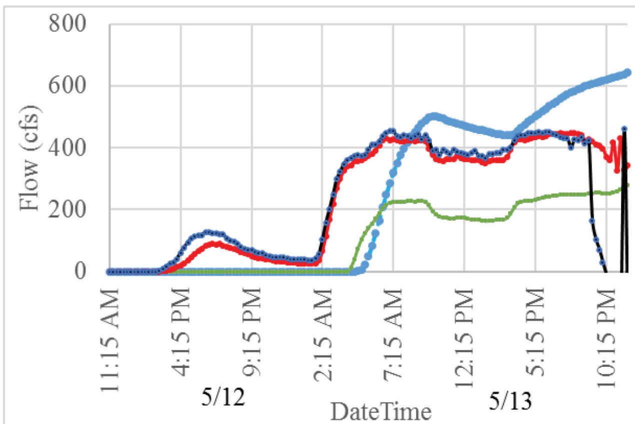

(b) Internal Boundary (weir)

Figure 5: Model results as flow at the (a) D/S boundary conditions and (b) internal boundary at weir for 1D and 2D models.

4.2 Limitations in 1D modeling and addressing them using 2D models

After breaching weir location, any flow into the storage area in the 1D model gets treated like a reservoir and does not get routed. This causes impractical depth increase in the storage area as shown in Fig. 6. Figure 6a is the water depth at the storage area after 2 h of breach and Fig. 6b is after 3.5 h of the breach. Since the storage area does not have a clear flow path, routing flow using 1D model is not feasible, which is an important limitation of 1D model. Figure 7 shows flow routing through the same storage area using a 2D model.

Another important limitation of 1D model is the inability to accurately model channel velocities. Figure 8a shows a meandering channel section and the cross section of 1D model. Figure 8b shows the velocity distribution as computed using flow distribution for 1D model. It shows that highest velocity magnitude is at the lowest section of the channel. However, for channel sections as shown, the velocity does not only depends on the cross section but also on the channel geometry. This can be modeled using a 2D model as shown in Fig. 8c.

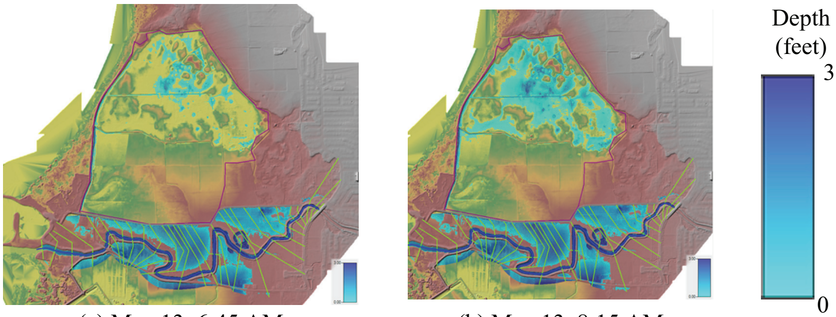

(a) May 13, 6:45 AM (b) May 13, 8:15 AM

Figure 6: Water level in the storage area using the 1D model.

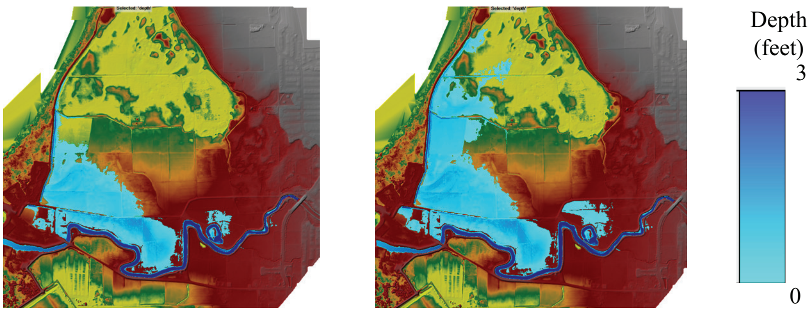

(a) May 13, 6:45 AM (b) May 13, 8:15 AM

Figure 7: Water level in the storage area using the 2D model.

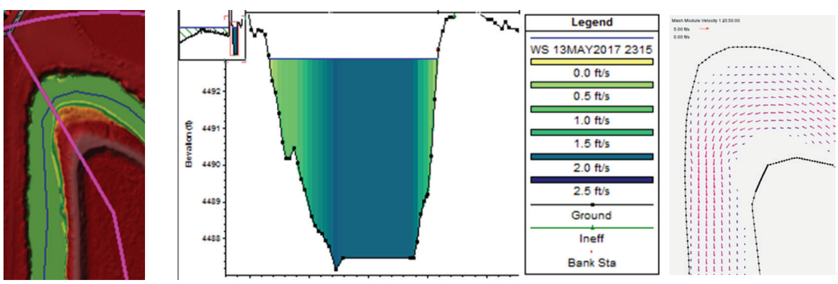

(a) (b) (c)

Figure 8: (a)Meandering channel section and velocity distribution in (b) 1D and (c) 2D.

4.3 Comparison of 2D models

This work used two different 2D models, HEC-RAS and SRH-2D which rely on the same mathematical model. However, since HEC-RAS can use an approximation scheme and the computation engines are different for these models, the performance and results vary for the models. These variations were different with different mesh types, sizes as well as computational time steps. The results in this section investigate on the differences in maximum water depth and velocity from these models.

Figure 9 shows the effect of grid sizes based on two HEC-RAS 2D models with grid sizes of 25 ft and 10 ft. Both these models were run with DW approximation approach with a computational time step of 5 s. The difference in maximum depth was higher in the storage area of the domain compared closer to the channel. Additionally, the extent of wet cells also increased with decreased cell size.

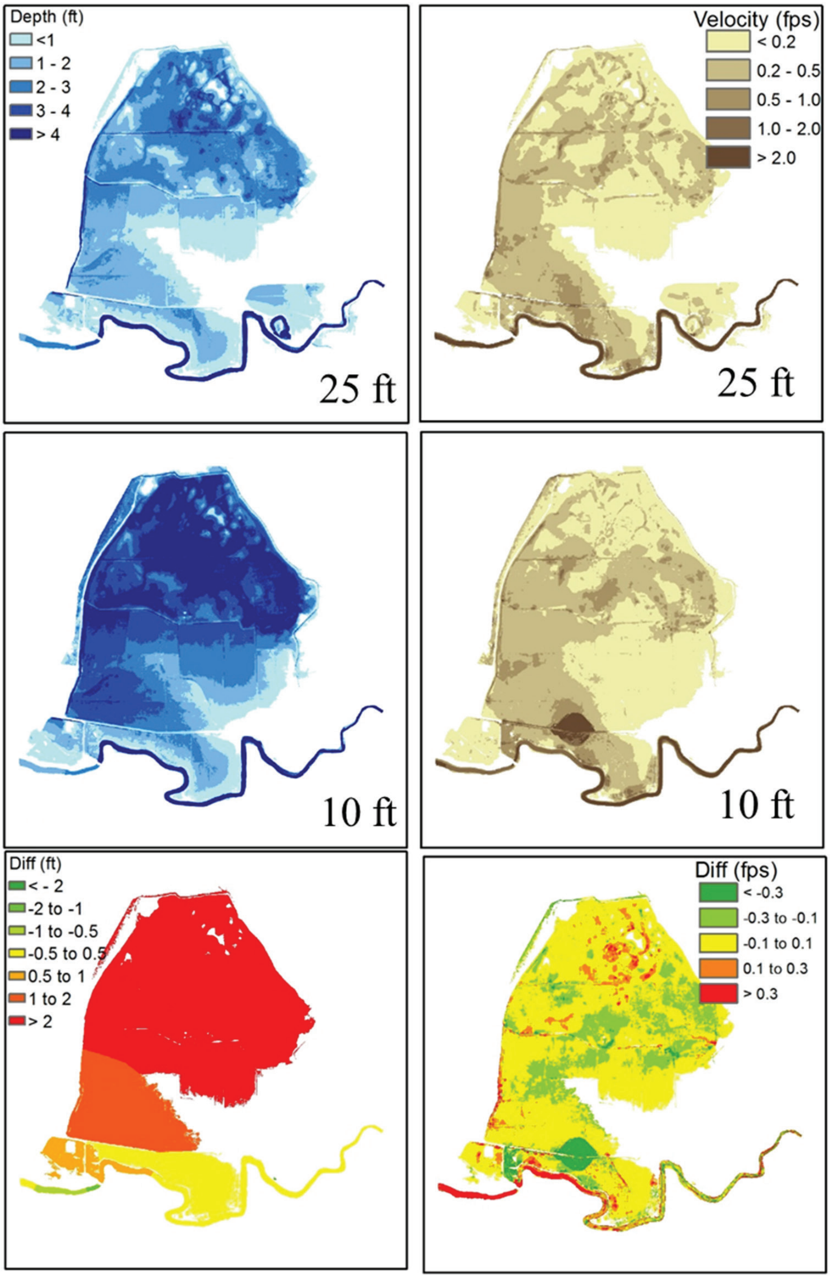

Figure 9: Effect of grid size on flow depth (left 3 panels) and flow velocity (right 3 panels).

Figure 10 shows the effect of modeling approach on maximum water depth and maximum velocity on two HEC-RAS 2D models each with grid size of 10 ft and computational time step of 5 s. The model which uses FM approach shows higher overall flow depth and lower velocity in the channel.

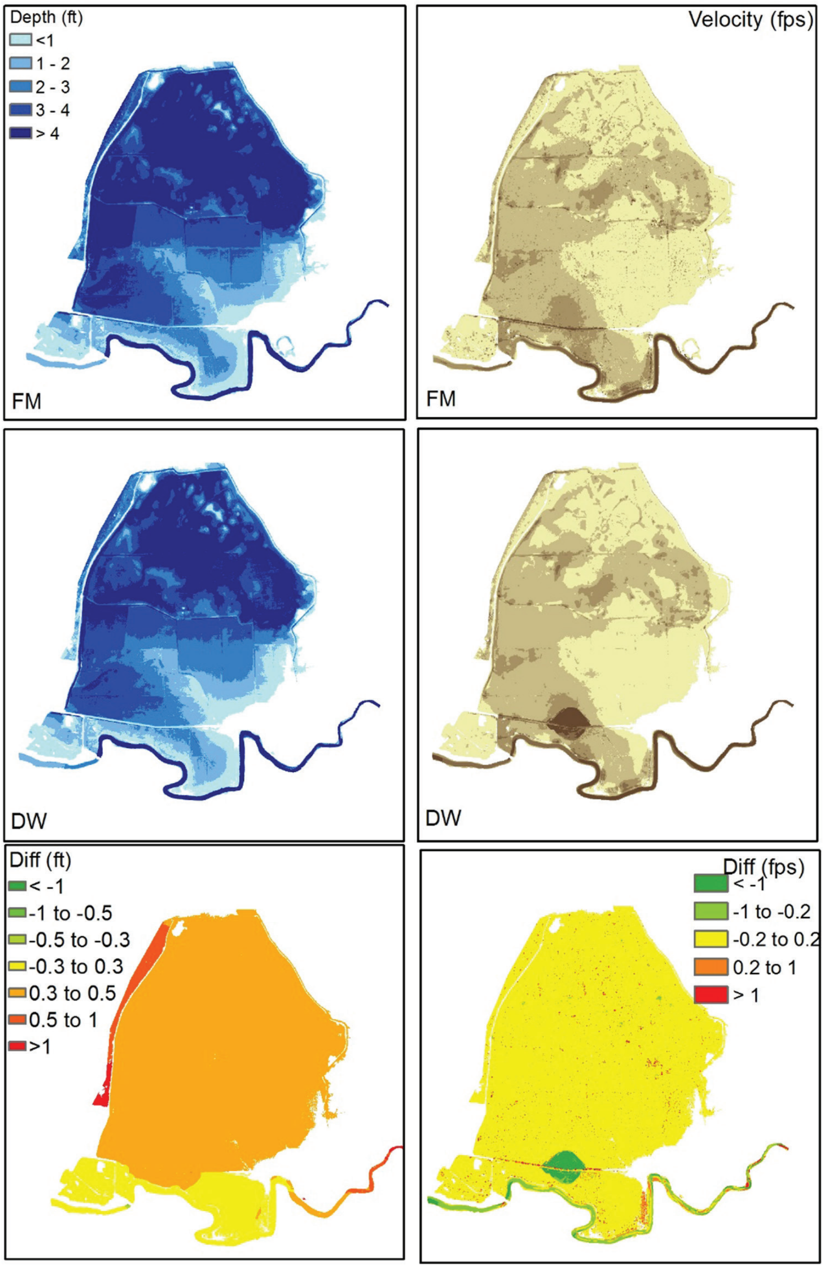

Figure 10: Effect of flood routing approach (diffusion wave (DW) and full momentum (FM)) on flow depth (left 3 panels) and flow velocity (right 3 panels).

Figure 11 shows the effect of grid optimization on maximum water depth on two SRH 2D models. Figure 11a shows fine gradient-based meshing with water depth and Fig. 11b shows optimized version of Fig. 11a. It can also be observed that there are differences in flooding extent as well as flood depths closer to the breach location.

The computational times were significantly different for these models. It ranged from 17 h for a 1-s time step SRH-2D model to 15 min for a 5-s time step HEC-RAS model.

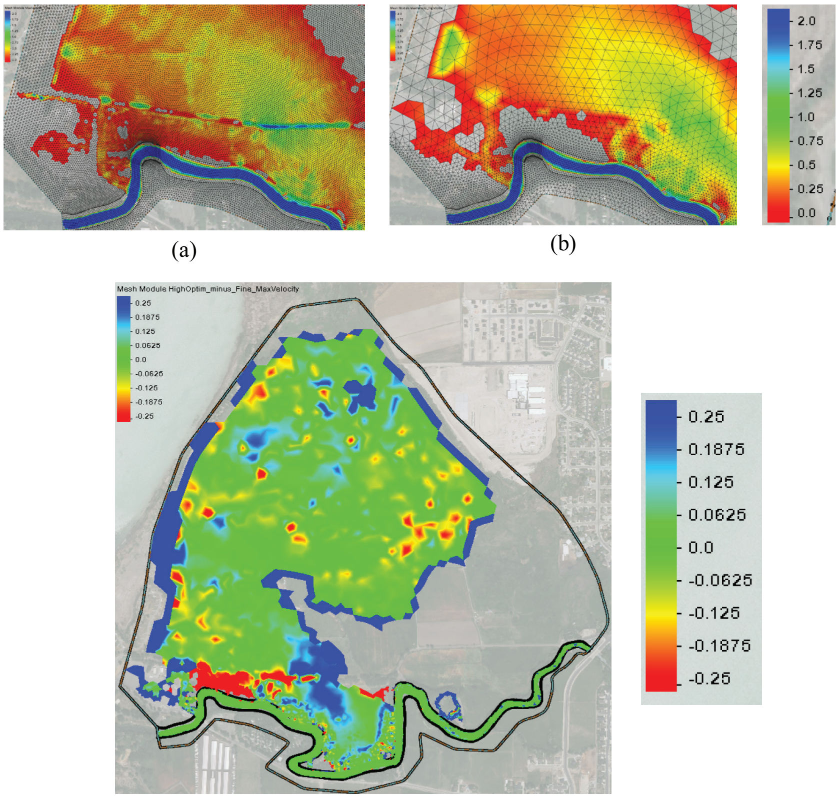

(c)

Figure 11: Effect of grid optimization on water depth in SRH-2D. (a) Using fine gradient-based mesh, (b) using optimized mesh, and (c) difference in water depths.

5 CONCLUSIONS

This work compared the performance of 1D flood models with 2D flood models and investigated the limitations in 1D that could be addressed using 2D models. Two popular flood modeling software, HEC-RAS, and SRH-2D were used with various modeling approaches, grid sizes, and time steps to understand their effects in flood routing. Some of these variations caused higher differences in flow depth and velocities while some did not significantly affect the results. However, the timings varied significantly within model runs and some of the models did not improve results even with longer run times.

We expect 2D models to be more prevalent in flood modeling studies, which require better understanding of their sensitivities and our work addressed some of them.

REFERENCES

[1] Qi, H. & Altinakar, M.S., A GIS-based decision support system for integrated flood management under uncertainty with two dimensional numerical simulations. *Environmental Modelling and Software*, **26**(**6**), pp. 817–821, 2011. https://doi.org/10.1016/j.envsoft.2010.11.006

[2] Tsakiris, G. & Bellos, V., 2014. A numerical model for two-dimensional flood routing in complex terrains. *Water Resources Management*, **28**(**5**), pp. 1277–1291. https://doi.org/10.1007/s11269-014-0540-3

[3] Tayefi, V., Lane, S.N., Hardy, R.R. & Yu, D., A comparison of one- and two-dimensional approaches to modelling flood inundation over complex upland floodplains. *Hydrological Processes*, **21(23)**, pp. 3190–3201, 2007. https://doi.org/10.1002/hyp.6523

[4] Bohorquez, P. & Darby, S.E., The use of one- and two-dimensional hydraulic modeling to reconstruct a glacial outburst flood in a steep alpine valley. *Journal of Hydrology*, **361**(**3–4**), pp. 240–261, 2008. https://doi.org/10.1016/j.jhydrol.2008.07.043

[5] Brown, R.A. & Pasternack, G.B., Comparison of methods for analyzing salmon habitat rehabilitation designs for regulated rivers. *River Research and Applications*, **25**(**6**), pp. 745–772, 2009. https://doi.org/10.1002/rra.1189

[6] Jones, K.E., Dahl, T.A. & Corum, Z.P., Modeled sedimentation in the lower White River county line levee setback, Washington State. U.S. Army Engineer Research and Development Center, ERDC/CHL TR-18-9, 2018.

[7] Gibson, S.A. & Pasternack, G.B., Selecting between one-dimensional and two-dimensional hydrodynamic models for ecohydraulic analysis. *River Research and Applications*, **32**(**6**), pp. 1365–1381, 2016. https://doi.org/10.1002/rra.2972

[8] Horritt, M.S. & Bates, P.D., Evaluation of 1D and 2D numerical models for predicting river flood inundation. *Journal of Hydrology*, **268**(**1–3**), pp. 87–99, 2002. https://doi.org/10.1016/s0022-1694(02)00121-x

[9] Fewtrell, T.J., Duncan, A., Sampson, C.C., Neal, J.C. & Bates, P.D., Benchmarking urban flood models of varying complexity and scale using high resolution terrestrial LiDAR data. *Physics and Chemistry of the Earth*, **36**(**7–8**), pp. 281–291, 2011. https://doi.org/10.1016/j.pce.2010.12.011

[10] Manfreda, S. Samela, C., Gioia, A. Consoli, G.G., Iacobellis, V., Giuzio, L. 2015. Flood-prone areas assessment using linear binary classifiers based on flood maps obtained from 1D and 2D hydraulic models. *Natural Hazards*, **79**(**2**), pp. 735–754. https://doi.org/10.1007/s11069-015-1869-5

[11] Zhang, T., Peng, L. & Feng, P., Evaluation of a 3D unstructured-mesh finite element model for dam-break floods. *Computers & Fluids*, **160**, pp. 64–77, 2018. https://doi.org/10.1016/j.compfluid.2017.10.013

[12] Brunner, G.W., *Hydraulic Reference Manual Version* 5.0. U.S. Army Corps of Engineers, Hydrologic Engineering Center, Davis, CA, 2016.

[13] Lai, Y.G., *SRH-2D version 2: Theory and User's Manual*. U.S. Department of Interior, U.S. Bureau of Reclamation Denver, CO. 2008.